AFRL-RX-WP-TP-2014-0067

ELECTRICAL, OPTICAL AND STRUCTURAL STUDIES OF INAS/INGASB VLWIR SUPERLATTICES

Gail J. Brown
AFRL/RXAN

JANUARY 2013
Interim Report

AIR FORCE RESEARCH LABORATORY
MATERIALS AND MANUFACTURING DIRECTORATE
WRIGHT-PATTERSON AIR FORCE BASE, OH 45433-7750
AIR FORCE MATERIEL COMMAND
UNITED STATES AIR FORCE

NOTICE AND SIGNATURE PAGE

Using Government drawings, specifications, or other data included in this document for any purpose other than Government procurement does not in any way obligate the U.S. Government. The fact that the Government formulated or supplied the drawings, specifications, or other data does not license the holder or any other person or corporation; or convey any rights or permission to manufacture, use, or sell any patented invention that may relate to them.

Qualified requestors may obtain copies of this report from the Defense Technical Information Center (DTIC) (http://www.dtic.mil)

AFRL-RX-WP-TP-2014-0067 HAS BEEN REVIEWED AND IS APPROVED FOR PUBLICATION IN ACCORDANCE WITH ASSIGNED DISTRIBUTION STATEMENT.

//SIGNED//
GAIL J. BROWN, Program Manager
Nanoelectronic Materials Branch
Functional Materials Division

//SIGNED//
DIANA M. CARLIN, Chief
Nanoelectronic Materials Branch
Functional Materials Division

//SIGNED//
KAREN R. OLSON, Deputy Chief
Functional Materials Division
Materials & Manufacturing Directorate

This report is published in the interest of scientific and technical information exchange and its publication does not constitute the Government's approval or disapproval of its ideas or findings.

REPORT DOCUMENTATION PAGE

Form Approved
OMB No. 0704-0188

1. REPORT DATE *(DD-MM-YY)*	2. REPORT TYPE	3. DATES COVERED *(From - To)*
January 2013	Final	1 July 2010 – 31 December 2012

4. TITLE AND SUBTITLE

ELECTRICAL, OPTICAL AND STRUCTURAL STUDIES OF INAS/INGASB VLWIR SUPERLATTICES

5a. CONTRACT NUMBER
In-House

5b. GRANT NUMBER

5c. PROGRAM ELEMENT NUMBER
62102F

6. AUTHOR(S)

Gail J. Brown, William C. Mitchel, Heather J. Haugan, Krishnamurthy Mahalingam, Mu J. Kim, and Frank Szmulowicz (AFRL/RX)
Said Elhamri (University of Dayton)

5d. PROJECT NUMBER
4348

5e. TASK NUMBER

5f. WORK UNIT NUMBER
X0A8 (PS112100)

7. PERFORMING ORGANIZATION NAME(S) AND ADDRESS(ES)

AFRL/RXAN
3005 Hobson Way
Wright-Patterson AFB, OH 45433-7734

University of Dayton
Department of Physics
Dayton, OH 45469

8. PERFORMING ORGANIZATION REPORT NUMBER

9. SPONSORING/MONITORING AGENCY NAME(S) AND ADDRESS(ES)

Air Force Research Laboratory
Materials and Manufacturing Directorate
Wright-Patterson Air Force Base, OH 45433-7750
Air Force Materiel Command
United States Air Force

10. SPONSORING/MONITORING AGENCY ACRONYM(S)
AFRL/RXAN

11. SPONSORING/MONITORING AGENCY REPORT NUMBER(S)
AFRL-RX-WP-TP-2014-0067

12. DISTRIBUTION/AVAILABILITY STATEMENT

Approved for public release; distribution is unlimited.

13. SUPPLEMENTARY NOTES

Approved by 88ABW Public Affairs Office: Case number 88ABW-2013-0115 on 11 January 2013. Report contains color.

14. ABSTRACT

InAs/InGaSb superlattice (SL) materials are an excellent candidate for infrared photodiodes with cut-off wavelengths beyond 15 µm, i.e. in the very long infrared wavelength (VLWIR) range. There are relatively few options for high performance infrared detectors to cover wavelengths longer than 15 µm, especially for operating temperatures above 15K. There are a variety of possible superlattice designs that will cover the VLWIR wavelength range, including designs with and without indium alloying of the GaSb layers. Transport modeling has shown that alloy scattering should not be a dominant factor in these superlattices so our focus is on designs with 25% indium in the gallium antimonide to achieve energy band gaps less than 50 meV with a superlattice period on the order of 68 Å. Similar to the work reported on InAs/GaSb LWIR and VLWIR superlattices, our designs employ InGaSb layers less than 7 monolayers in width. While the superlattice designs are strain balanced to the GaSb substrate, care was also taken to minimize strain spikes in the interfacial regions. High resolution transmission electron microscope images were analyzed to create strain mapping profiles of the SL layers and interfaces. By focusing on a narrow set of VLWIR SL designs, the deposition parameters for the molecular beam epitaxial SL growth could be carefully optimized.

15. SUBJECT TERMS

superlattice (SL), molecular beam epitaxy, very long infrared wavelength (VLWIR)

16. SECURITY CLASSIFICATION OF:			17. LIMITATION OF ABSTRACT:	18. NUMBER OF PAGES	19a. NAME OF RESPONSIBLE PERSON (Monitor)
a. REPORT	b. ABSTRACT	c. THIS PAGE			Gail J. Brown
Unclassified	Unclassified	Unclassified	SAR	24	19b. TELEPHONE NUMBER *(Include Area Code)* (937) 255-9854

TABLE OF CONTENTS

Section **Page**

List of Figures ii

List of Tables ii

1 Introduction 1

2 Sample Fabrication/Design 2

3 Structural Characterization 3

4 Optical Characterization 7

5 Electronic Transport Measurements 10

6 Electronic Transport Modeling 13

7 Summary 15

8 References 16

List of Acronyms, Abbreviations, and Symbols 19

LIST OF FIGURES

Figure **Page**

1 A HRTEM Image of Sample A Showing the First Few Layers in the InGaSb/InAs Superlattice Near the GaSb Substrate 4

2 Strain Analysis of Sample A Showing (a) the Map of the Strain Tensor, ε_{yy}, Parallel to the Growth Direction and (b) a Plot of the Strain Profile Averaged Parallel to the Interface, over the Boxed Region in (a) 5

3 Strain Analysis of Sample D Showing (a) the Map of the Strain Tensor, ε_{yy}, Parallel to the Growth Direction and (b) a Plot of the Strain Profile Averaged Parallel to the Interface, over the Boxed Region in (a) 6

4 Photoresponse Spectrum at 8K for Sample A 8

5 Comparison of the Photoresponse Spectra of Sample A and Sample D taken under the same Experimental Conditions at 8K 9

6 Carrier Concentration Versus Inverse Temperature for Sample A 11

7 Mobility Versus Temperature for Sample A 11

8 The Mobility as a Function of Temperature for a Lightly N-Type GaSb Substrate 12

9 Mobility Versus Temperature, Linear T Scale, for Alloyed and Unalloyed Superlattices. Sample B (o) and Sample C (x) 12

10 The calculated horizontal and vertical mobilities, using $\Lambda = 200$ Å and $\Delta = 1.65$ Å, and the measured horizontal mobility as a function of temperature for the 48.1 Å InAs/20.4Å GaSb SL 14

11 The temperature dependence of IRS-limited, horizontal mobilities for a 48.1 Å InAs/20.4 Å GaSb SL as a function of correlation length 14

LIST OF TABLES

Table **Page**

1 Sample Designs, SL Period Measured by X-Ray Diffraction and the Optical Band Gap Energy Determined by the Photoresponse Spectra 2

1. Introduction

InAs/InGaSb superlattice (SL) materials are an excellent candidate for infrared photodiodes with cut-off wavelengths beyond 15 μm, i.e. in the very long infrared wavelength (VLWIR) range. There are relatively few options for high performance infrared detectors to cover wavelengths longer than 15 μm, especially for operating temperatures above 15K. There are a variety of possible superlattice designs that will cover the VLWIR wavelength range, including designs with and without indium alloying of the GaSb layers.[1] For homogeneous InGaSb alloys transport modeling found that alloy scattering should be negligible for electrons.[2] In addition, there can be benefits for incorporating InGaSb into the VLWIR SL design, such as a higher molecular beam epitaxy (MBE) growth temperature which should reduce point defects in the InGaSb, simpler interfaces with the continuous indium flux, suppressed Auger recombination rates, and larger absorption coefficients due to thinner periods in these designs.

Our focus is on designs with 25% indium in the gallium antimonide to achieve energy band gaps less than 50 meV with a superlattice period on the order of 68 Å. Similar to the work reported on InAs/GaSb LWIR and VLWIR superlattices[3-5], our designs employ InGaSb layers less than 7 monolayers in width. While the superlattice designs are strain balanced to the GaSb substrate, care was also taken to minimize strain spikes in the interfacial regions. High resolution transmission electron microscope images were analyzed to create strain mapping profiles of the SL layers and interfaces. By focusing on a narrow set of VLWIR SL designs, the deposition parameters for the molecular beam epitaxial SL growth could be carefully optimized.

The electrical and optical properties of the VLWIR superlattices were characterized by variable temperature Hall Effect measurements and by infrared photoresponse spectra. The photoresponse spectra consistently showed a band gap energy of 47 ± 3 meV for the samples studied and a 50% cutoff wavelength at ~ 19 μm. The repeatability of these very narrow band gap superlattices over multiple sample depositions, and while some growth parameters were being adjusted, shows the tight control obtainable with molecular beam epitaxy. Narrow band gap designs are very sensitive to small changes in layer widths.[6] Variable temperature Hall effect measurements found that the mobility of electrons in the SL was ~10,000 cm^2/Vs below 80 K and was relatively constant in magnitude.

2. Sample Fabrication/design

The VLWIR SLs were grown by molecular beam epitaxy using standard metal effusion cells for Ga and In, and valved cracker cells for As and Sb. In order to minimize cross contamination of the anion fluxes, the V/III flux ratio was set at a minimum of 3 for both the InAs and GaSb depositions. The grow rates were: 1.20 Å/s for GaSb, 1.6 Å/s for $In_{0.25}Ga_{0.75}Sb$, and 0.33 Å/s for InAs. The SL stack (0.5 µm) and the GaSb buffer layer (0.5 µm) were deposited on lightly doped n-type GaSb (100) wafers at a temperature of 410 °C for InAs/GaSb and 430 °C for InAs/InGaSb. For the InGaSb based VLWIR SL we used a design of 47.0 Å InAs/21.5 Å $In_{0.25}Ga_{0.75}Sb$ as calculated by Grein *et al.*[7] to have a band gap of 80 meV at 40K. The interface between the InAs and InGaSb layers was not intentionally controlled by shutter sequence to be either InSb-like or GaAs-like. The residual strain of the two InGaSb based SLs remained small and slightly compressive at +0.2 % (samples A and B). For the GaSb based VLWIR SL we used a design, based on our previous studies[8], of 48 Å InAs/20.5 Å GaSb including the controlled InSb-like interfaces. The controlled interfaces are necessary to strain balance the lattice mismatched InAs. With the controlled InSb-like interfaces the net strain of sample C was close to zero. The structural parameters of the samples, such as SL period, residual strain, and individual layer thickness were confirmed by high-resolution transmission electron microscopy (HRTEM) and high-resolution x-ray diffraction (HRXRD) measurements. A summary of the intended SL designs, measured HRXRD SL period, and measured band gap energy determined from the onset of the photoresponse spectra is given in Table 1.

Table 1. Sample designs, SL period measured by x-ray diffraction and the optical band gap energy determined by the photoresponse spectra.

Sample	InAs (Å)	GaSb (Å)	In (%)	IF (Å)	Period (Å)	E_g (meV)
A	47	21.5	25	0	68	46
B	47	21.5	25	0	68	44
C	46.5	18	0	1.5/2.5	69	63
D	47	21.5	25	0	68.5	45

3. Structural Characterization

In this section we present results from a high-resolution transmission electron microscope (HRTEM) study, wherein the superlattices were imaged using recent techniques based on aberration-corrected TEM. As reported in recent studies[9-12], the improved spatial resolution achieved by aberration correction offers the capability for quantitative image analysis, particularly with regard to determining the composition and strain profiles across interfaces at atomic resolution. In the present study an investigation is performed to examine the strain distribution in these superlattices. A detailed description of the methods adopted, including the techniques for image acquisition and analysis and its application to InAs-GaSb superlattices, are presented in a recent report.[12] In brief, the superlattices were imaged using a Titan 80-300 TEM equipped with an (image) spherical-aberration corrector, and strain analysis of the HRTEM images was performed using the peak-pair method.[13] The analysis was performed such that the strain components ε_{xx} was parallel to the interface (along [011]) and ε_{yy} along the growth direction ([100]).

Figure 1 is a HRTEM image of sample A, showing the individual layers in the superlattice near the substrate region, where the $In_{0.25}Ga_{0.75}Sb$ and InAs layers appear dark and bright respectively. From these images the average superlattice period was determined be 67.6 ± 0.3 Å, with an average layer thickness of 24.1±1.6 Å for InAs and 44.1±1.2 Å for $In_{0.25}Ga_{0.75}Sb$. The results from strain analysis of the HRTEM images are shown in Fig. 2, where Fig. 2(a) is a map of the strain tensor ε_{yy}, and Fig. 2(b) is a profile of its distribution across individual layers, averaged parallel to the interface within the area indicated in the figure. It is observed that the InGaSb layers (bright yellow regions) are in compressive strain, which is consistent with the In content (x=0.25) in these layers, and that the InAs layers (bright green) are in tensile strain of about 0.01, which is in agreement with theoretical calculations of based on published values of elastic constants. The InGaSb-on-InAs and InAs-on-InGaSb interfaces are seen to exhibit strain inversion so that the overall strain in these regions is negligible.

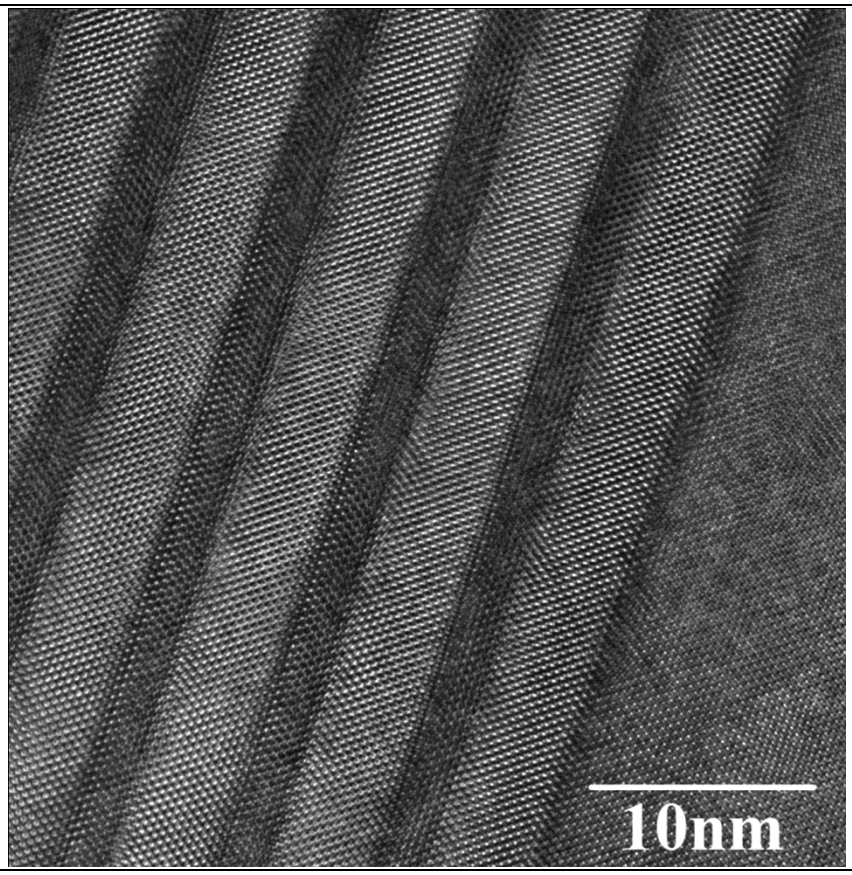

Figure 1. A HRTEM image of sample A showing the first few layers in the InGaSb/InAs superlattice near the GaSb substrate.

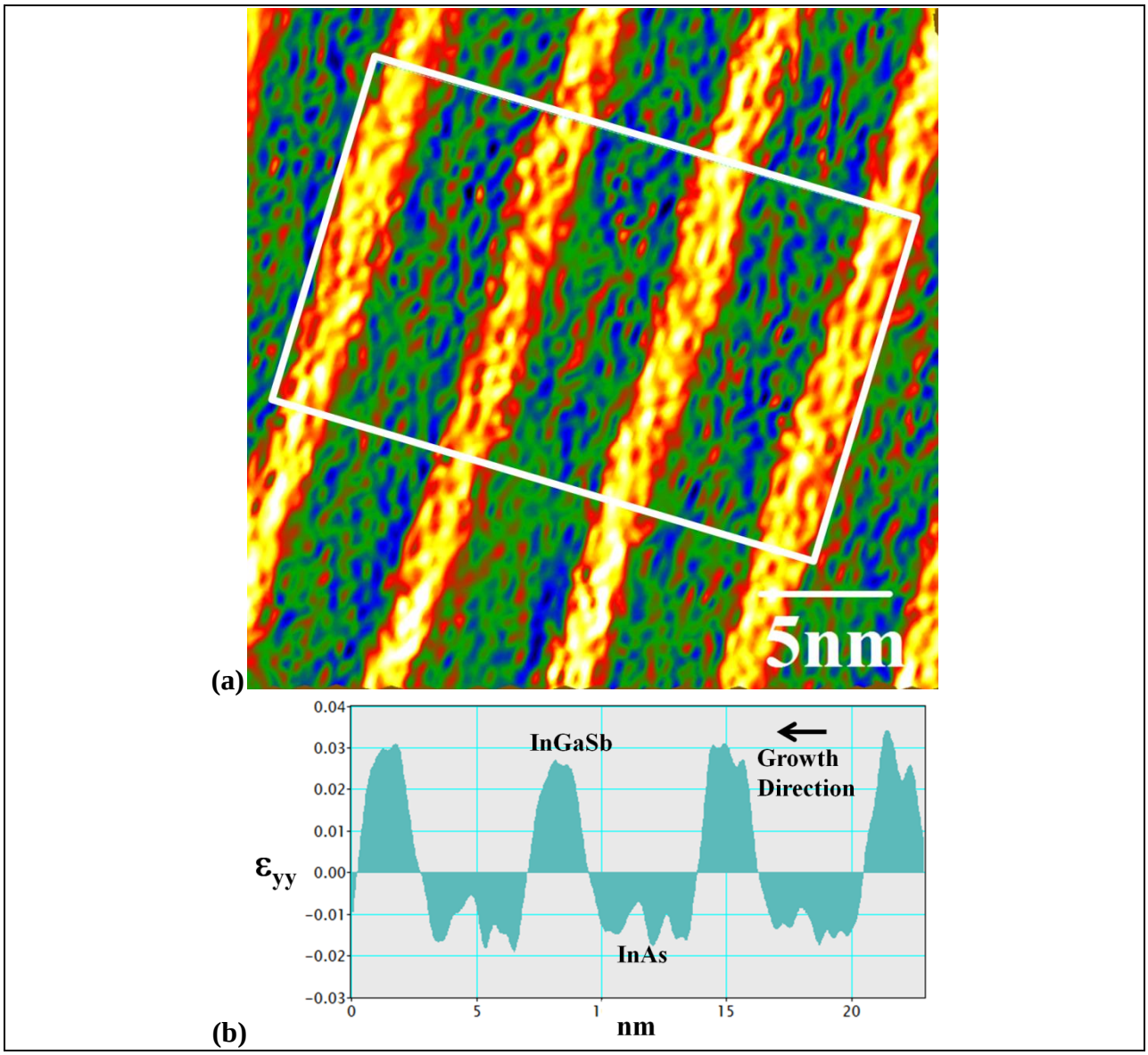

Figure 2 Strain analysis of sample A showing (a) the map of the strain tensor, ε_{yy}, parallel to the growth direction and (b) a plot of the strain profile averaged parallel to the interface, over the boxed region in (a).

While for the most part the observations for sample A were similar to other superlattices reported in recent studies[11,12,14], it is important to emphasize that the strain distribution profiles at the InGaSb-on-InAs interfaces for this sample were distinctly different from those observed in earlier studies. To elaborate further, we present results from a recent study[14] which pertain to sample D in Table 1. Although samples A and D are similar in design, the HRXRD profiles for the two samples showed that sample A was in compressive strain with respect to the GaSb substrate (ε = +0.17%), whereas sample D was closely lattice matched (ε = 0.0%). Fig. 3a shows the strain map for sample D, and Fig. 3b the profile of ε_{yy}, averaged parallel to the interface within the boxed region in Fig. 3a. The profile in Fig. 3b shows sharp negative spikes at the InGaSb-on-InAs interface (denoted by arrows), which are not observed in the strain profile for

sample A (Fig. 2b). The negative spikes indicate that this interface is in tensile strain and that the dominant bond type at this interface is Ga-As. In both samples the InGaSb layers have a peaked compressive strain of around 3%, while the regions corresponding to the InAs-on-InGaSb interfaces are nearly strain balanced due to strain inversion. Based on the values of overall strain for the two samples determined by HRXRD, it is clear that the tensile strain at the InGaSb-on-InAs interface is important for achieving strain balance in the alloyed superlattice. As observed in earlier reports, the maps of ε_{xx} for both of the samples (A & D) showed negligible values indicating that these interfaces were coherent with the GaSb substrate.

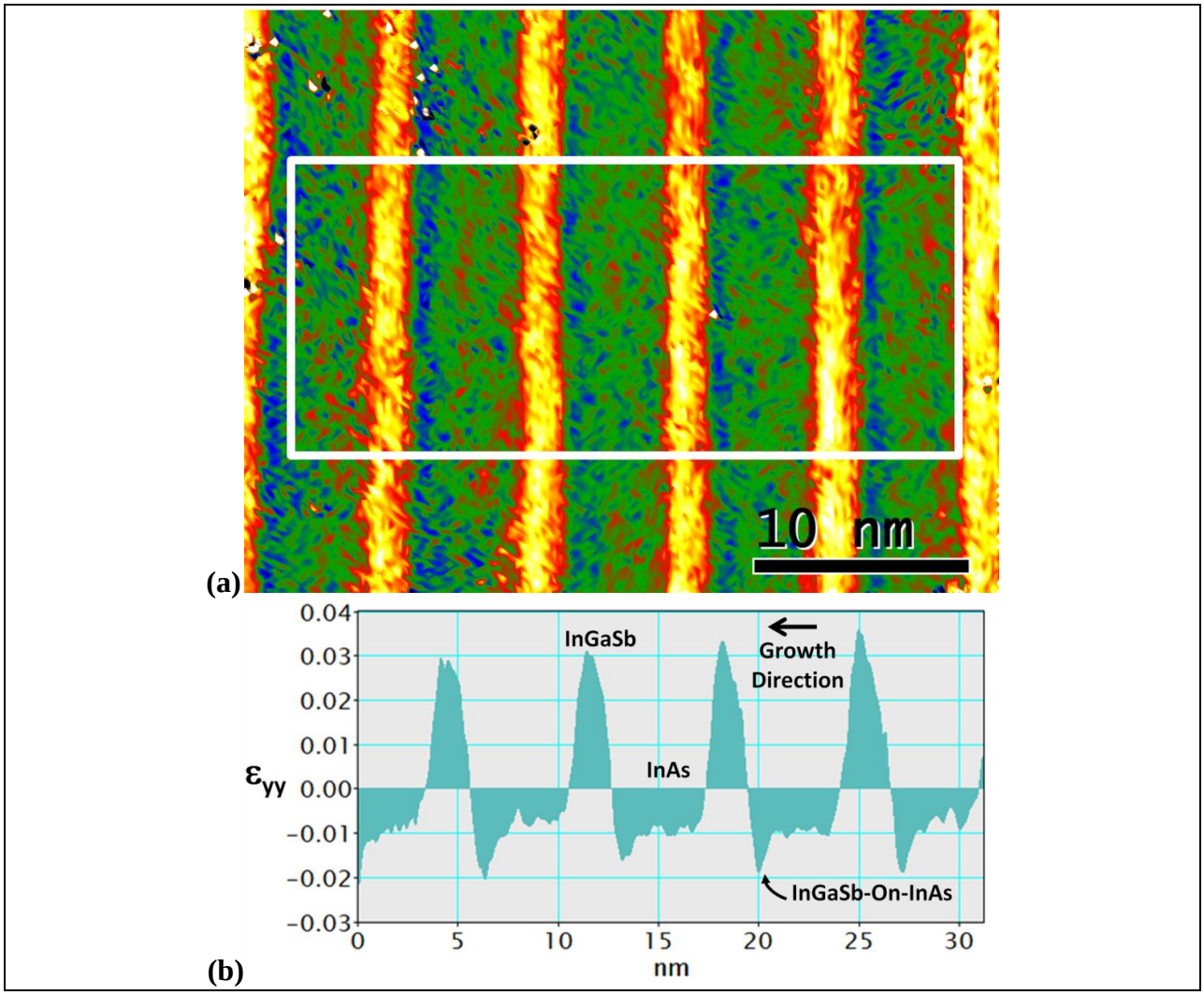

Figure 3 Strain analysis of sample D showing (a) the map of the strain tensor, ε_{yy}, parallel to the growth direction and (b) a plot of the strain profile averaged parallel to the interface, over the boxed region in (a).

4. Optical Characterization

The photoresponse spectra were measured on the SL samples using the photoconductive mode where indium strip contacts were applied to top of the SL stack. The samples were typically 5 mm by 10 mm in optical area with ~3 mm between the two strip contacts on the long sides of the rectangular samples. Care was taken to keep the indium strips away from the edge of the samples. Due to the less than 1 kΩ resistance of the samples at low temperature the spectra were collected in a current bias mode versus using a voltage bias. Spectra were measured from 8 K up to 80 K for these narrow band gap samples. Since an FTIR spectrometer was used to collect the spectra, the photoresponse does not have quantitative units and is instead expressed in arbitrary units. However, a comparison can be made between samples run under the same experimental conditions to measure improvements to the SL deposition conditions.

The photoresponse spectrum of a typical VLWIR superlattice (sample A) is shown in Fig. 4. The band gap is determined by drawing a line down the photoresponse (PR) onset and finding the energy for zero PR. This avoids the band tail issue. The measured band gap energies are shown in Table 1. For a much larger sample set than these few samples the average band gap energy for the same superlattice design was 47 ± 3 meV. The measured band gap energies are lower than the theoretically predicted value of 80 meV by Grein *et al.*[7] and the cutoff wavelength of 19 μm, measured at the point where the PR intensity has dropped by 50%, is longer. The HRXRD and cross-sectional TEM measurements confirm that the SL samples grown were very close to the intended design so that the discrepancy between theory and experiment must originate in the modeling.

A good photoresponse signal was measured despite the fact that the SL total thickness was only ~3 % of the VLWIR photon wavelength. For a maximum absorption coefficient of 2500 cm^{-1} at 5.6 μm, the absorption quantum efficiency would only be ~7 % in the mid-infrared in a single pass, and about half this value by $\lambda > 12.5$ μm. The heavy fringing on the long wavelength portion of the spectrum is not noise but a result of multiple internal reflections through the substrate/buffer/superlattice stack. The lightly n-type GaSb wafers do have significant infrared transparency.[15] As shown in Fig. 4, the SL has its maximum response over a wide wavelength range up to ~15 μm.

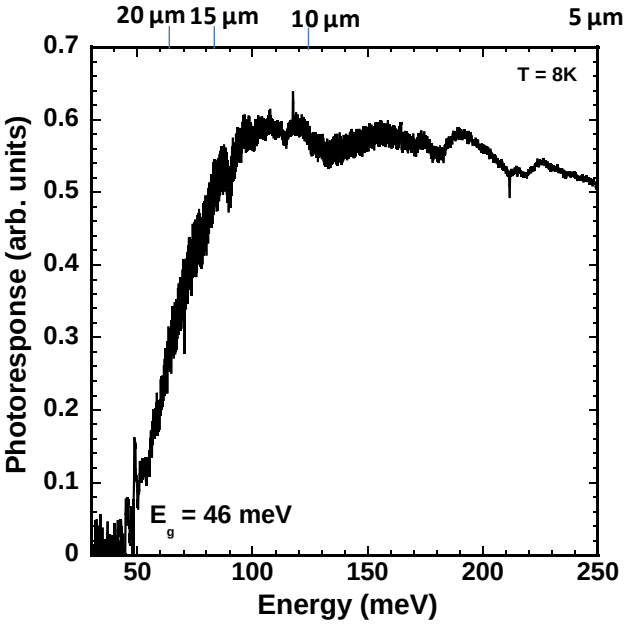

Figure 4. Photoresponse spectrum at 8K for sample A.

The impact of reducing the interface strain on the superlattice photoresponse was studied. For this study we compared sample A and sample D used in the HRTEM study. These two samples were grown about a week apart such that the overall MBE conditions were nearly the same except for the arsenic beam equivalent pressure which was set ~30% higher for sample D. A comparison of the two photoresponse spectra measured at 8 K is shown in Figure 5. Overall the two spectra are very similar with the same onset energy and 50% cutoff wavelength. There is a difference in the magnitude of the photoresponse such that sample D produced about 80% of the signal of sample A. Our run to run variation of photoresponse intensity when remounting and retesting the same sample is on the order of 10% or less. So the intensity difference between these two samples is larger than experimental variation. Still, the intensity difference is not very large so the impact of a negative strain spike at the InGaSb-on-InAs interface may be relatively minor.

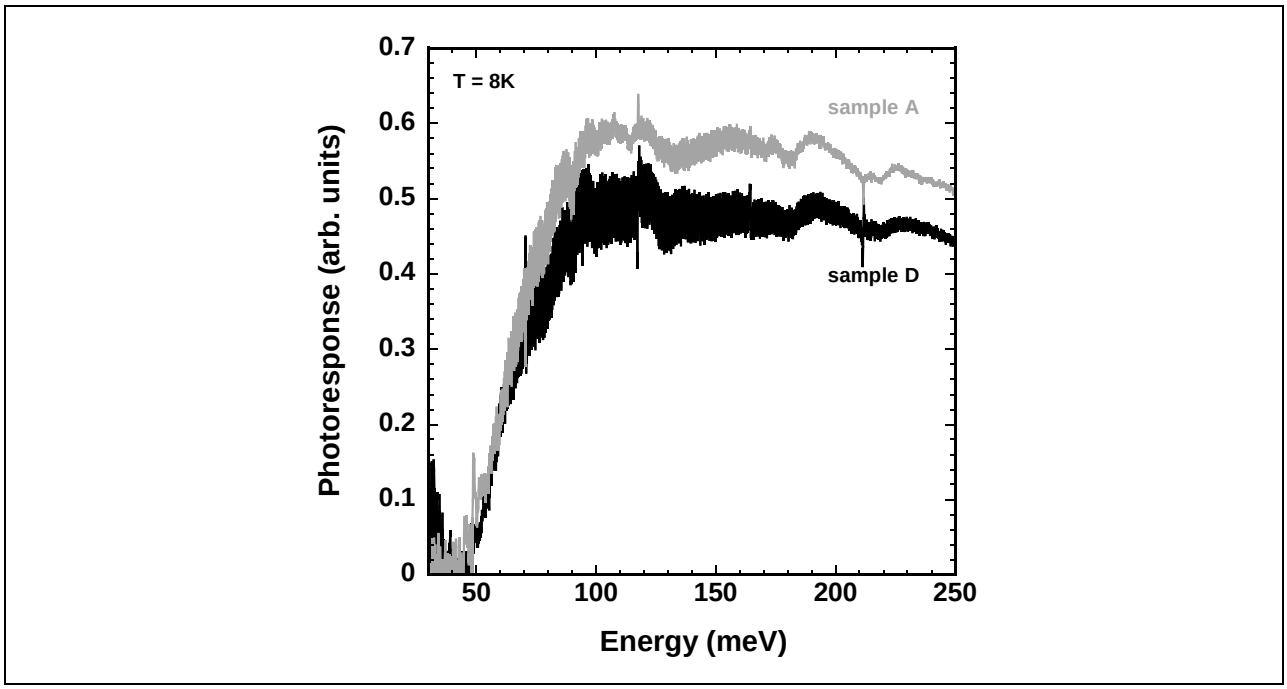

Figure 5. Comparison of the photoresponse spectra of sample A and sample D taken under the same experimental conditions at 8 K.

5. Electronic Transport Measurements

The use of lightly n-type GaSb substrates for the superlattice deposition provides the opportunity to measure the superlattice transport properties without any contribution from the substrate.[16] The substrate had a carrier concentration of 2 x 10^{16} cm^{-3} at 10 K and mobility below 4000 cm^2/Vs in the temperature range from 5 K to 300 K. Given that the n-type substrate electrons do not freeze out, and their mobilities remain finite at low temperatures, the charge carrier contributions from the substrate would be expected to dominate the Hall transport measurements, as happens for the standard n-type GaSb wafers that are more heavily doped with tellurium. However, the combination of a lightly n-type substrate with the intrinsically p-type GaSb buffer layer provides electrical isolation of the VLWIR superlattice over a wide temperature range. This eliminates the need for inserting AlGaSb barrier layers, which can roughen the subsequent superlattice layers, trying to grow a comparable quality SL on semi-insulating GaAs versus GaSb, or trying to remove the substrate and measure properties without negatively impacting the SL material in the process.

The in-plane transport properties of sample A are shown in Figs. 6 and 7. Figure 6 shows the carrier concentration vs. inverse temperature data while Fig. 7 shows mobility vs. temperature. The sample is n-type at all temperatures which is typical for VLWIR SL designs where InAs is the major portion of the SL period. The electron sheet concentration is relatively independent of temperature below 80 K with value of 6.4 x10^{11} cm^{-2} at 10 K. Above that temperature the concentration increases rapidly with increasing temperature. This is most likely thermal activation of free carriers, possibly across the superlattice bandgap. Activation from some other layer in the structure cannot be ruled out at this time. The mobility in Fig. 7 also shows distinctly different behavior above and below 80 K. Above this temperature it shows behavior similar to bulk semiconductors, as seen in the lightly n-type GaSb in Fig. 8, with decreasing mobility from 140 K to 80 K, similar to ionized impurity scattering, followed by a decreasing mobility reminiscent of optical phonon scattering at temperatures above 140 K. Below 80 K the mobility is only weakly dependent on temperature. Among the possible low temperature scattering mechanisms two are particularly important for SLs, interface roughness[11] (IRS) and alloy scattering[2] (AS). For a constant carrier concentration IRS has been proposed to be independent of temperature[17] while AS is expected to go as temperature to the minus one half power[2]. To investigate the impact of alloy scattering two samples were grown to nearly identical specifications except that sample B had alloyed InGaSb while sample C used GaSb. The temperature dependences of the mobilities of these two samples from 10 K to 80 K are shown in Fig. 9 along with a solid line representing a $T^{-1/2}$ dependence. It is clear from Fig. 9 that alloying the GaSb layer does not significantly affect either the magnitude or the temperature dependence of the electron mobility at low temperatures. For thin GaSb or InGaSb layers, there is significant wave function overlap/penetration of the electron wave function into the alloyed layer so alloy scattering needs to be considered.

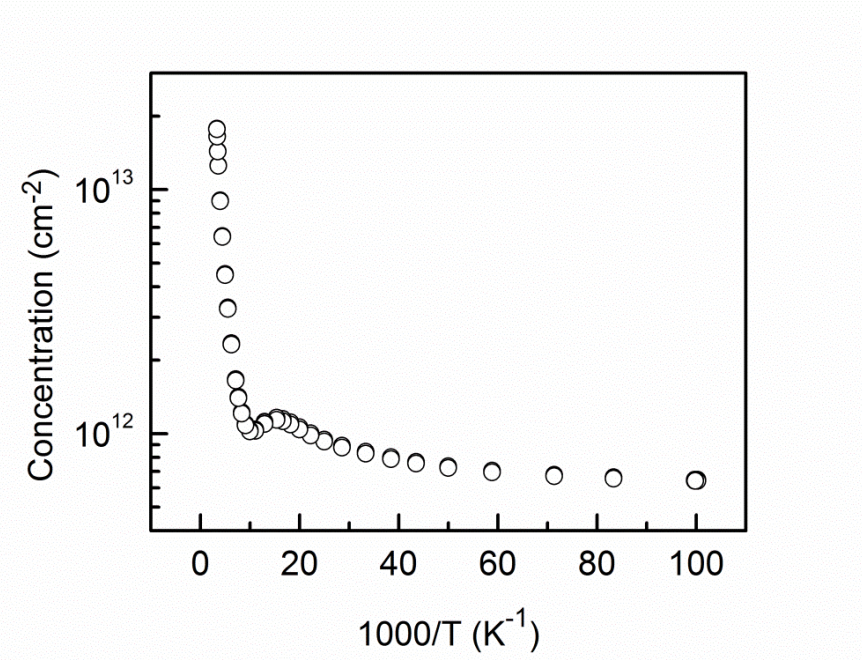

Figure 6. Carrier concentration versus inverse temperature for sample A.

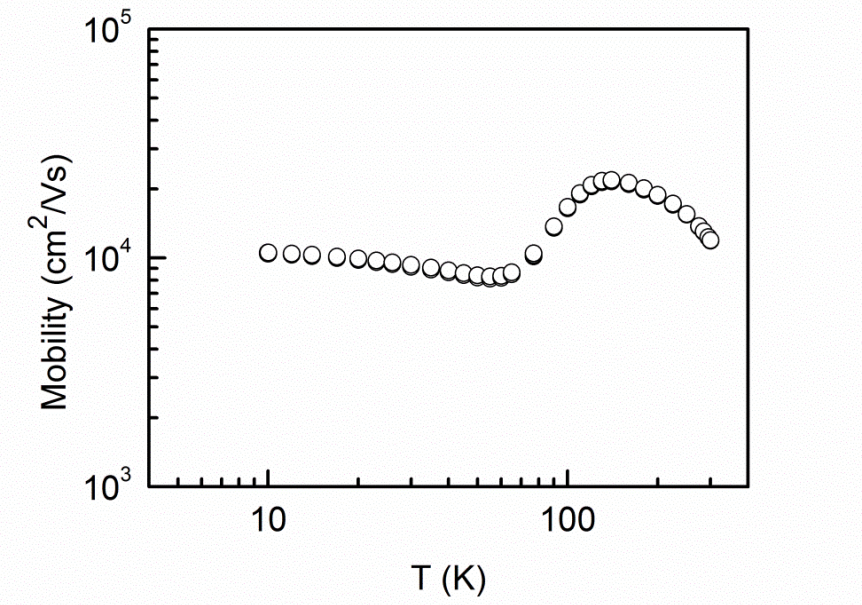

Figure 7. Mobility versus temperature for sample A.

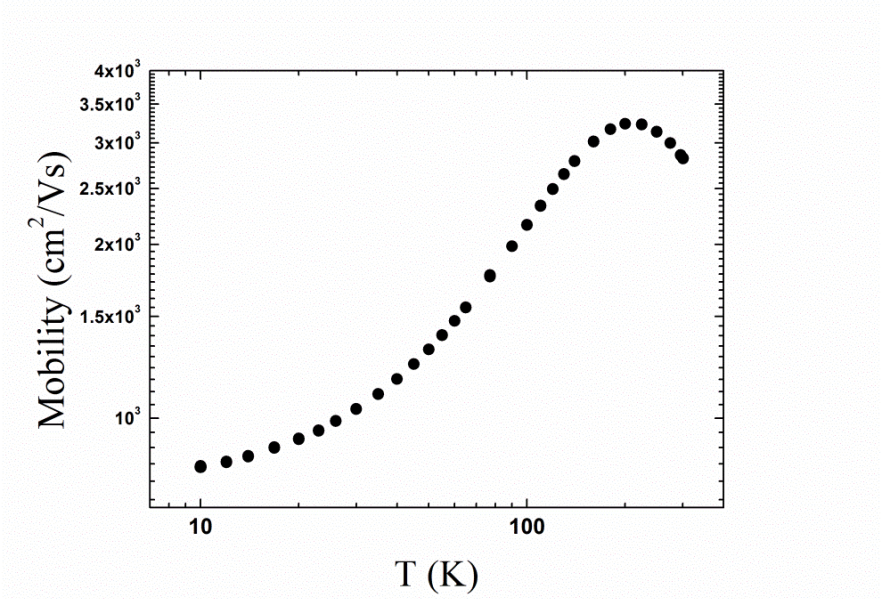

Figure 8. The mobility as a function of temperature for a lightly N-type GaSb substrate.

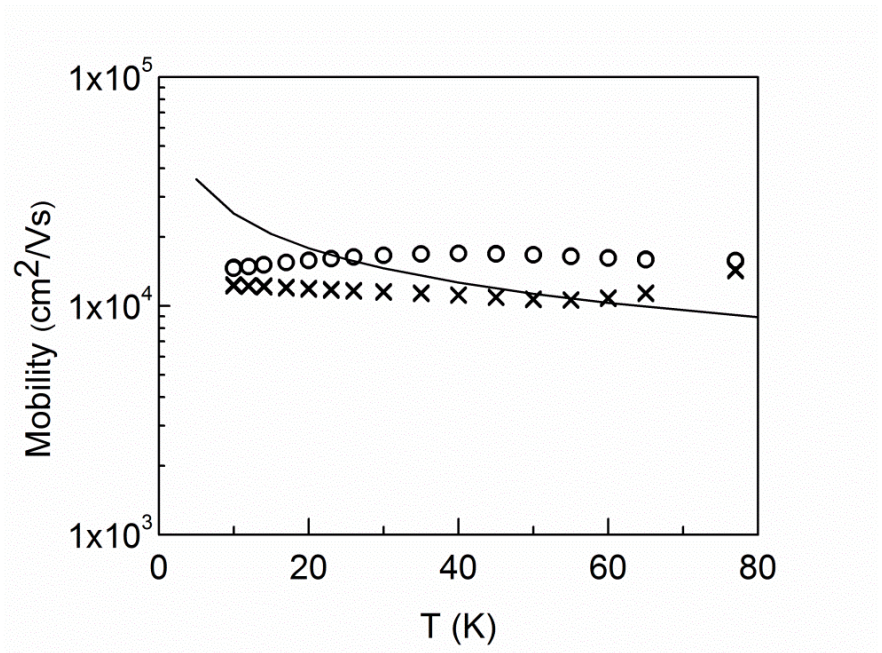

Figure 9. Mobility versus temperature, linear T scale, for alloyed and unalloyed superlattices. Sample B (○) and sample C (x).

6. Electronic Transport Modeling

In this section we calculate temperature-dependent perpendicular and horizontal interface roughness scattering (IRS)-limited mobilities[18,19] for sample C by expanding on our earlier work on low temperature transport in InAs/GaSb SLs.[20,21] The present treatment is specialized to electron transport, following the details provided in the low-temperature calculation[18-20] : the electron band structure, $\varepsilon(k_z)$, and wave functions in the growth direction k_z are calculated using the 3x3 envelope-function approximation (EFA). However, the electron and hole masses, $m_{||}$, in the in-plane direction are found from the full 8x8 EFA.[22] Temperature-dependent lattice constants, band gap energies, and other physical data for InAs and GaSb are taken from Vurgaftman *et al*.[23] Hence, the band structure, the carrier density, and carrier screening[24-27] are fully temperature dependent. The source of IRS scattering rates are fluctuations, Δ, in InAs layer width, which are characterized by the lateral correlation length of interface fluctuations Λ.[28-33] Using the calculated electron and heavy-hole energy bands for sample C, the chemical potential was calculated as a function of temperature. Then the Boltzmann equation was solved for the relaxation rates, which were then used to calculate the electron mobilities. The calculated horizontal and vertical mobilities and the measured horizontal mobility for sample C are shown in Fig. 10. The value of Λ=200 Å best fits the shape of the measured horizontal mobility. The magnitude of the measured mobility is best fit using the vertical roughness parameter Δ = 1.62 Å, if both interfaces are equally rough. In the temperature interval shown, the horizontal mobility is relatively flat, while the vertical mobility decreases. The overall agreement between experimental and theoretical horizontal mobility is good.

While the calculations highlighted in Fig. 10 show a relatively small temperature dependence of the IRS limited horizontal mobility, changes in the selection of Δ and Λ can lead to IRS limited mobilities that exhibit a much stronger temperature dependence as shown in Fig. 11. For these calculations the same sample C design parameters were used, but Δ was set to 3 Å and Λ was varied from 30 Å to 300 Å. Therefore, the relatively constant mobilities we see consistently below 80 K in a variety of superlattice samples with different designs may have a different explanation rather than simply IRS limited behavior.

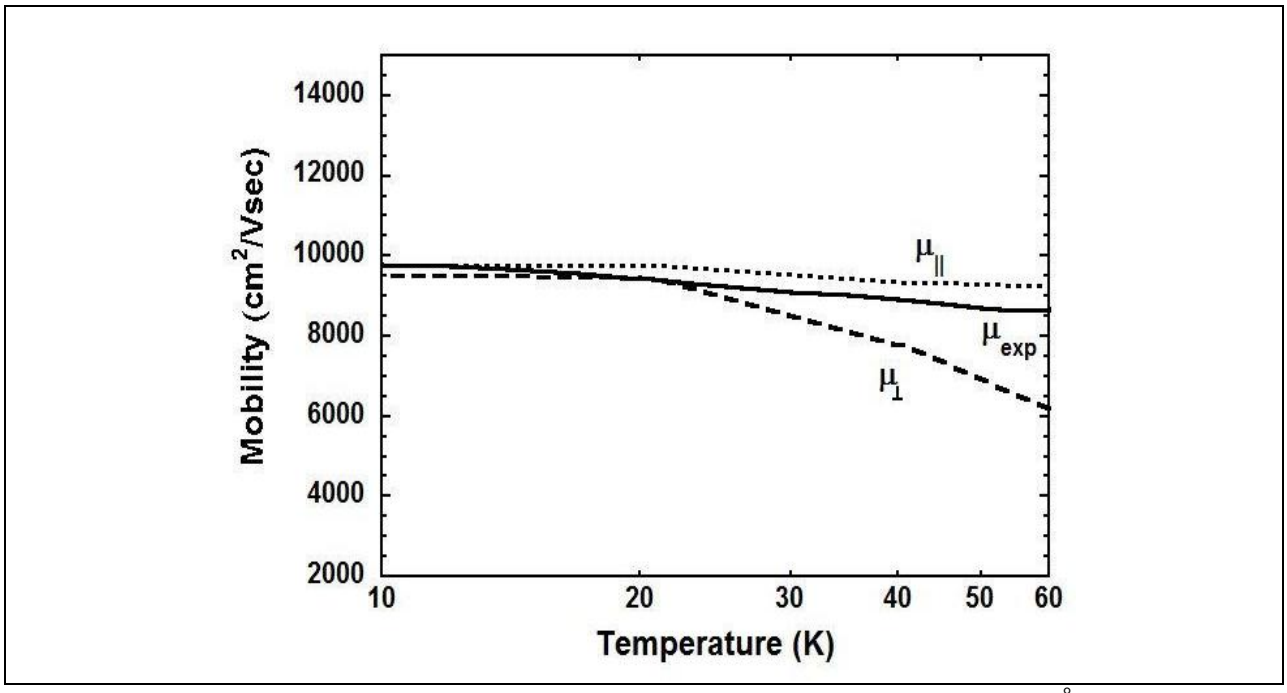

Figure 10. The calculated horizontal and vertical mobilities, using Λ = 200 Å and Δ = 1.65 Å, and the measured horizontal mobility as a function of temperature for the 48.1 Å InAs/20.4Å GaSb SL

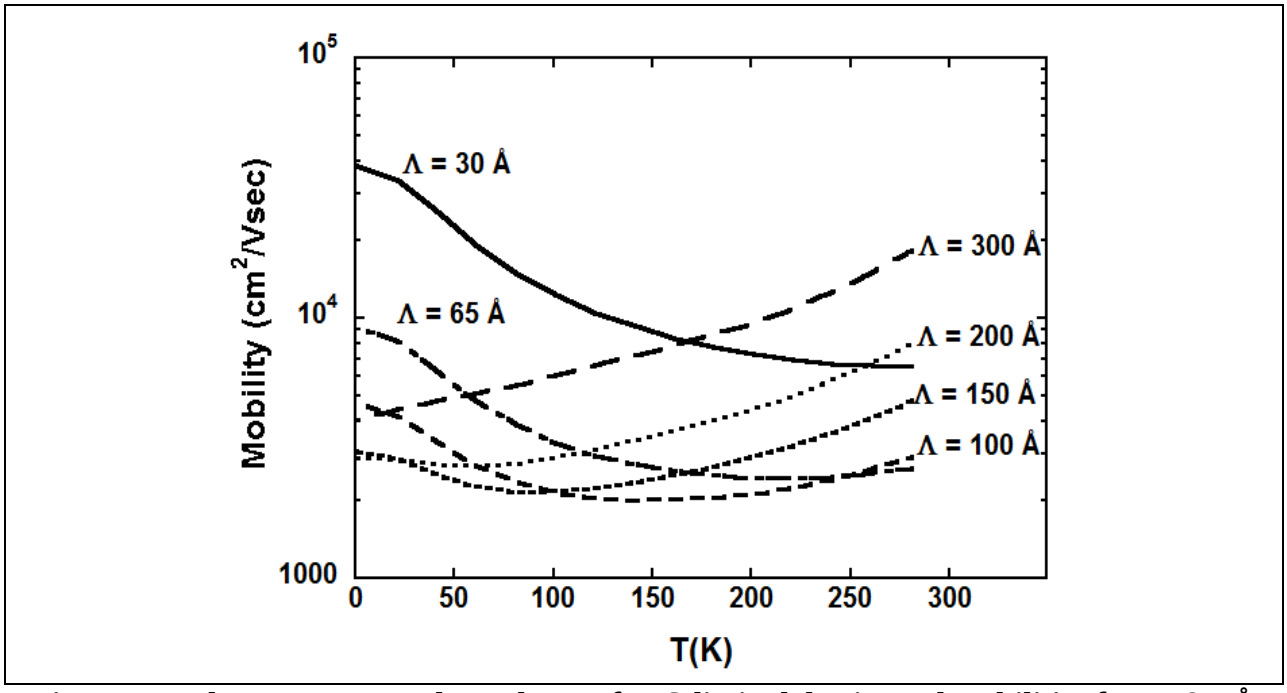

Figure 11. The temperature dependence of IRS-limited, horizontal mobilities for a 48.1 Å InAs/20.4 Å GaSb SL as a function of correlation length.

7. Summary

There are many advantages for using InGaSb alloys in the design and growth of VLWIR InAs/(In)GaSb superlattices: higher MBE growth temperature, simpler interface growth and mitigation of strain spikes, reduced Auger rates[7] and higher quantum efficiency. Alloy scattering of charge carriers was shown not to be a factor the electronic transport so there are no disadvantages to incorporating the indium into the GaSb layers. Variable temperature Hall effect measurements found that the in-plane mobility of electrons in the SL was ~10,000 cm^2/Vs below 80 K and was relatively constant in magnitude. Theoretical modeling of the vertical transport, in the interface roughness scattering limit, found the electron mobility perpendicular to the SL layers was nearly equivalent the in-plane mobility below 20 K but then had a stronger temperature dependence and dropped to ~6,000 cm^2/Vs by 60 K. The vertical transport is an important parameter in photodiode performance.

A quantitative analysis of the strain distribution was performed at the atomic scale by aberration corrected TEM. The results highlight the role of strain distribution at the InGaSb-on-InAs interfaces in the superlattices examined in this study. Capability for these measurements is important for understanding HRXRD data, particularly with regard to interpreting effective superlattice strain measurements.

The photoresponse spectra of the 47.0 Å InAs/21.5 Å $In_{0.25}Ga_{0.75}Sb$ SL design consistently had band gap energy of 47 ± 3 meV and a 50% cutoff wavelength at ~ 19 µm. The repeatability of these very narrow band gap superlattices over multiple sample depositions, and while some growth parameters were being adjusted, confirms the tight control obtained with our molecular beam epitaxy system. By focusing on a narrow set of VLWIR SL designs, the deposition parameters for the MBE SL growth can be carefully optimized.

8. References

1 E. R. Heller, K. Fischer, F. Szmulowicz and F. L. Madarasz, "Superlattice parameters for optimum absorption in $InAs/In_xGa_{1-x}Sb$ superlattice infrared detectors," *J. Appl. Phys.* **77**, 5739-5746 (1995).

2 J. J. Tietjen and L. R. Weisberg, "Electron mobility in $GaAs_{1-x}P_x$ alloys," *Appl. Phys. Lett.* **7**(10), 261-263 (1965).

3 P-Y Delaunay, B.-M. Nguyen, D. Hoffman, and M. Razeghi, "320x256 infrared focal plane array based on type-II InAs/GaSb superlattice with a 12 μm cutoff wavelength," *Proc. SPIE* **6542**, 654204-1 – 654204-10 (2007).

4 Y. Wei, A. Gin, M. Razeghi and G. J. Brown, "Advanced InAs/GaSb superlattice photovoltaic detectors for very long wavelength infrared applications," *Appl. Phys. Lett.* **80**(18) 3262 – 3264 (2002).

5 Y. Wei, A. Gin, M. Razeghi and G. J. Brown, "Type-II InAs/GaSb superlattice photovoltaic detectors with cutoff wavelength approaching 32 μm," *Appl. Phys. Lett.* **81**(19) 3675 – 3677 (2002).

6 F. Szmulowicz, E. R. Heller, K. Fischer and F. L. Madarasz, "Optimization of absorption in $InAs/In_xGa_{1-x}Sb$ superlattices for long-wavelength infrared detection," *Superlattices and Microstructures* 17(4), 373-379 (1995).

7 C. H. Grein, W. H. Lau, T. L. Harbert and M. E. Flatte, "Modeling of very long infrared wavelength InAs/GaInSb strained layer superlattice detectors," *Proc. SPIE* **4795**, 39-43 (2002).

8 H. J. Haugan, G. J. Brown and L. Grazulis, "Effect of interfacial formation on the properties of very long wavelength InAs/GaSb superlattics," *J. Vac. Sci. Technol.* B **29**(3) 03C101-1 – 03C101-5 (2011).

9 K. Mahalingam, K. G. Eyink, G. J. Brown, D. L. Dorsey, C. F. Kisielowski and A. Thust, "Compositional analysis of mixed –cation-anion III-V semiconductor interfaces using phase retrieval high-resolution transmission electron microscopy," *J. Microscopy* **230**, 372-381 (2008).

10 K. Mahalingam, K. G. Eyink, G. J. Brown, D. L. Dorsey, C. F. Kisielowski, and A. Thust, "Quantifying stoichiometry of mixed anion-cation III-V semiconductor interfaces at atomic resolution," *Appl. Phys. Lett.* **88**, 091904-091906 (2006).

11 K. Mahalingam, H. J. Haugan, G. J. Brown, K. G. Eyink, and B. Jiang, "Quantitative strain analysis of interfaces in InAs/GaSb superlattices by aberration-corrected HAADF-STEM," *Proc. SPIE* **8268**, 826831-1– 826831-5 (2012).

12 K. Mahalingam, H. J. Haugan, G. J. Brown, K. G. Eyink, "Quantitative analysis of interfacial strain in InAs/GaSb superlattices by aberration-corrected HRTEM and HAADF-STEM," *Ultramicroscopy* (2012 in press)), http://dx.doi.org/10.1016/j.ultramic.2012.09.005

13 P. L. Galindo, S. Kret, A. M. Sanchez, J-Y. Laval, A. Yanez, J. Pizarro, E. Guerrero, T. Ben, and S. I. Molina, "The peak pairs algorithm for strain mapping from HRTEM images," *Ultramicroscopy* **107**, 1186-1193 (2007).

14 H. J. Haugan, G. J. Brown, S. Elhamri, W. C. Mitchel, K. Mahalingam, et al. "Impact of growth temperature on InAs/GaInSb strained layer superlattices for very long wavelength infrared detection," *App.Phys.Lett.* **101**, 171105-1 – 171105-4 (2012).

15 L.P. Allen, P. Flint, G. Dallas, D. Bakken, K. Blanchat, G. J. Brown, S.R. Vangala, W.D. Goodhue and K. Krishnaswami, "GaSb substrates with extended IR wavelength for advanced space based applications," *Proc. SPIE* **7298**, 72983P-1 – 72983P-7 (2009).

16 H. J. Haugan, G. J. Brown, S. Elhamri, S. Pacley, B. V.Olson, and T. F. Boggess, "Post growth annealing study on long wavelength infrared InAs/GaSb superlattices," J. Appl. Phys. 111, 053113-1 – 053113-4 (2012).

17 C. A. Hoffman , J. R. Meyer, E. R. Youngdale, F. J. Bartoli and R. H. Miles "Interface roughness scattering in semiconducting and semimetallic InAs-$Ga_{1-x}In_xSb$ superlattices," *Appl. Phys. Lett.* **63**(16), 2210-2212 (1993).

18 F. Szmulowicz, H. Haugan, S. Elhamri, and G. J. Brown, "Calculation of the temperature dependence of the vertical and horizontal mobiities in InAs/GaSb superlattices," *Infr. Phys. & Techn*. **56**, 76-79 (2013).

19 F. Szmulowicz and G. J. Brown, "Calculation of interface roughness scattering-limited vertical and horizontal mobilities in InAs/GaSb superlattices as a function of temperature," *J. Appl. Phys*. (2013 in press).

20 F. Szmulowicz and G. J. Brown, "Calculation of the vertical and horizontal electron mobilities in InAs/GaSb superlattices," *Appl. Phys. Lett*. **98**, 182105-1 – 182105-3 (2011).

21 F. Szmulowicz, H. J. Haugan, S. Elhamri, and G. J. Brown, "Calculation of vertical and horizontal mobilities in InAs/GaSb superlattics," *Phys. Rev. B* **84**, 155307-1– 155307-14 (2011).

22 F. Szmulowicz, H. J. Haugan, and G. J. Brown, "Effect of interfaces and the spin-orbit band on the band gaps of InAs/GaSb superlattices beyond the standard envelope-function approximation," *Phys. Rev. B* **69**, 155321-1– 155321-17 (2004).

23 I. Vurgaftman, J. R. Meyer, and L. R. Ram-Mohan, "Band parameters for III–V compound semiconductors and their alloys**,**" *J. Appl. Phys*. **89**, 5815-5875 (2001).

24 B. Laikhtman and R. A. Kiehl, "Theoretical hole mobility in a narrow Si/SiGe quantum well," *Phys. Rev. B* **47**, 10515-10527 (1993).

25 David K. Ferry and Stephen M. Goodnick, "Quantum Confined Systems," in *Transport in Nanostructures*, Cambridge Press, Cambridge, UK (1977).

26 P. F. Maldague, "Many-body corrections to the polarizability of the two-dimensional electron gas," *Surf. Sci.* **73**, 296-302 (1973).

27 Y. Okuyama and N. Fakuda, "Electron-phonon interactions in modulation-doped $A_{lx}Ga_{1-x}As$/GaAs heterojunctions," *Phys. Rev. B* **40**, 9744-9750 (1989).

28 S. Mori and T. Ando, "Electronic properties of a semiconductor superlattice II. Low temperature mobility perpendicular to the superlattice," *J. Phys. Soc. Japan* **48** (3), 865-873 (1980).

29 I. Dharssi and P. N. Butcher, "The effect of phonon confinement on perpendicular electron transport in a GaAs /GaAlAs superlattice," *J. Phys. Condens. Matter* **2**, 119-125 (1990).

30 F. Aristone, P. Gassot, J. F. Palmier, D. K. Maude, B. Goutiers, J. L. Gauffier, J. C. Portal, and F. Mollot, "Probing the interface fluctuations in semiconductor superlattices using a magneto-transport technique," *Superlattices Microstructructures* **5**, 225-228 (1994).

31 J. Q. You, L. Zhang, and Q. B. Yang, "Longitudinal magnetotransport in long-period semiconductor superlattices," *Phys. Rev. B* **55**, 15757-15761 (1997).

32 G. J. Warren and P. N. Butcher, "A mobility calculation for a GaAs/GaAlAs superlattice," *Semicond. Sci. Technol*. **1**, 133-136 (1986).

33 G. Etemadi and J. F. Palmier, "Effect of interface roughness on non-linear vertical transport in GaAs/AlAs superlattices," *Solid State Commun*. **86**, 739-743 (1993).

LIST OF ACRONYMS, ABBREVIATIONS, AND SYMBOLS

Acronym	Definition
SL	Superlattice
VLWIR	Very Long Infrared Wavelength
MBE	Molecular Beam Epitaxy
HRTEM	High-Resolution Transmission Electron Microscopy
HRXRD	High-Resolution X-Ray Diffraction
FTIR	Fourier Transform Infrared
PR	Photoresponse
IRS	Interface Roughness Scattering
EFA	Envelope-Function Approximation